

1 **TITLE:**

2 High-throughput Expression and Purification of Human Solute Carriers for Structural and
3 Biochemical Studies

4

5 **AUTHORS AND AFFILIATIONS:**

6 Sagar Raturi¹, Huanyu Li¹, Yung-Ning Chang², Andreea Scacioc¹, Tina Bohstedt¹, Alejandra
7 Fernandez-Cid¹, Adam Evans¹, Patrizia Abrusci¹, Abilasha Balakrishnan¹, Tomas C. Pascoa¹, Didi
8 He¹, Gamma Chi¹, Nanki Kaur Singh¹, Mingda Ye¹, Anna Li¹, Leela Shrestha¹, Dong Wang¹, Eleanor
9 P. Williams¹, Nicola A. Burgess-Brown^{1*}, Katharina L. Dürr^{1*}, Vera Puetter^{2*}, Alvaro Ingles-Prieto^{3*},
10 David B. Sauer^{1*}

11

12 ¹Centre for Medicines Discovery, Nuffield Department of Medicine, University of Oxford, Oxford,
13 UK

14 ²Nuvisan ICB GmbH, Berlin, Germany

15 ³CeMM Research Center for Molecular Medicine of the Austrian Academy of Sciences, Vienna,
16 Austria

17

18 **Email addresses of the co-authors:**

19 Sagar Raturi (sagar.raturi@cmd.ox.ac.uk)
20 Huanyu Li (huanyu.li@cmd.ox.ac.uk)
21 Yung-Ning Chang (yung-ning.chang@nuvisan.com)
22 Andreea Scacioc (andreea.scacioc@gmail.com)
23 Tina Bohstedt (tina.bohstedt@embl.de)
24 Alejandra Fernandez-Cid (Alejandracanteli@gmail.com)
25 Adam Evans (Axe943@student.bham.ac.uk)
26 Patrizia Abrusci (pabrusci@exscientia.co.uk)
27 Abilasha Balakrishnan (abilasha02@icloud.com)
28 Tomas C. Pascoa (tomas.pascoa@cmd.ox.ac.uk)
29 Didi He (didi.he@hotmail.com)
30 Gamma Chi (gamma.chi@cmd.ox.ac.uk)
31 Nanki Kaur Singh (n.singh20@imperial.ac.uk)
32 Mingda Ye (martin.ye@cmd.ox.ac.uk)
33 Anna Li (anna.li@gtc.ox.ac.uk)
34 Leela Shrestha (leelashre@gmail.com)
35 Dong Wang (dong.wang@cmd.ox.ac.uk)
36 Eleanor P. Williams (eleanor.williams@cmd.ox.ac.uk)

37

38 **Corresponding authors:**

39 Nicola A. Burgess-Brown (nburgessbrown@exactsciences.com)
40 Katharina L. Dürr (katharina.duerr@omass.com),
41 Vera Puetter (Vera.Puetter@nuvisan.com)
42 Alvaro Ingles-Prieto (AInglesprieto@cemm.oeaw.ac.at)
43 David B. Sauer (david.sauer@cmd.ox.ac.uk)

44

45 **KEYWORDS:**

46 Solute carrier, transporter, cloning, protein expression, membrane protein

47

48 **SUMMARY:**

49 Structural and biochemical studies of human membrane transporters require milligram
50 quantities of stable, intact, and homogeneous protein. Here we describe scalable methods to
51 screen, express, and purify human solute carrier transporters using codon-optimized genes.

52

53 **ABSTRACT:**

54 Solute carriers (SLCs) are membrane transporters that import and export a range of endogenous
55 and exogenous substrates, including ions, nutrients, metabolites, neurotransmitters, and
56 pharmaceuticals. Despite having emerged as attractive therapeutic targets and markers of
57 disease, this group of proteins is still relatively underdrugged by current pharmaceuticals. Drug
58 discovery projects for these transporters are impeded by limited structural, functional, and
59 physiological knowledge, ultimately due to the difficulties in the expression and purification of
60 this class of membrane-embedded proteins. Here, we demonstrate methods to obtain high-
61 purity, milligram quantities of human SLC transporter proteins using the codon-optimized gene
62 sequences. In conjunction with a systematic exploration of construct design and high-throughput
63 expression, these protocols ensure the preservation of the structural integrity and biochemical
64 activity of the target proteins. We also highlight critical steps in the eukaryotic cell expression,
65 affinity purification, and size-exclusion chromatography of these proteins. Ultimately, this
66 workflow yields pure, functionally active, and stable protein preparations suitable for high-
67 resolution structure determination, transport studies, small-molecule engagement assays, and
68 high-throughput *in vitro* screening.

69

70 **INTRODUCTION:**

71 Membrane proteins have long been targets for researchers and pharmaceutical industries alike.
72 Of these, the solute carriers (SLCs) are a family of over 400 secondary transporter genes encoded
73 within the human genome ¹. These transporters are involved in the import and export of
74 numerous molecules, including ions ², neurotransmitters ³, lipids ⁴⁻⁷, amino acids ⁸, nutrients ⁹⁻
75 ¹¹, and pharmaceuticals ¹². With such a breadth of substrates, these proteins are also implicated
76 in a range of pathophysiology through the transport of toxins ¹³, transport and inhibition by
77 drugs of abuse ^{14, 15}, or deleterious mutations ¹⁶. Bacterial homologs have served as prototypes
78 for the fundamental transport mechanism of several SLC families ¹⁷⁻²⁵. In contrast to human
79 proteins, prokaryotic orthologs are often better expressed in the well-understood *Escherichia coli*
80 expression system ^{26, 27} and are more stable in the smaller detergents which yield well-ordered
81 crystals for X-ray crystallography ²⁸. However, sequence and functional differences complicate
82 the use of these distantly-related proteins for drug discovery ^{29, 30}. Consequently, direct study of
83 the human protein is often needed to decipher the mechanism of action of drugs targeting SLCs
84 ³¹⁻³⁵. While the recent advances in Cryo-electron Microscopy (Cryo-EM) have enabled structural
85 characterization of SLCs in more native-like conditions ^{36, 37}, difficulty in expressing and purifying
86 these proteins remains a challenge for developing targeted therapeutics and diagnostics.

87

88 To alleviate this challenge, the RESOLUTE consortium (re-solute.eu) has developed resources and

89 protocols for the large-scale expression and purification of human SLC-family proteins³⁸. Starting
90 with codon-optimized genes, we have developed methods for the high-throughput cloning and
91 screening of SLC constructs. These methods were systematically applied to the whole family of
92 SLCs, the genes were cloned into the BacMam viral expression system, and the protein expression
93 was tested in human cell lines³⁹ based on previously described methods for high-throughput
94 cloning and expression testing⁴⁰. In summary, the *SLC* gene is cloned from the pDONR221
95 plasmid into a pHTBV1.1 vector. This construct is subsequently used to transpose the gene of
96 interest into a bacmid vector for transfecting insect cells, which includes a cytomegalovirus
97 promoter and enhancer elements for expression in mammalian cells. The resulting baculovirus
98 can be used to transduce mammalian cells for the expression of the target SLC protein.

99
100 We further developed standardized methods for large-scale expression and stable purification of
101 selected SLCs (**Figure 1**). This protocol includes multiple checkpoints to facilitate effective
102 troubleshooting and minimize variability between experiments. Notably, routine monitoring of
103 protein expression and localization, as well as small-scale optimization of purification conditions
104 for individual targets, were aided by Strep and Green Fluorescent Protein (GFP) tags^{41, 42}.

105
106 Ultimately, these chemically pure and structurally homogeneous protein samples can be used for
107 structural determination by X-ray crystallography or Cryo-Electron Microscopy (Cryo-EM),
108 biochemical target-engagement assays, immunization for binder generation, and cell-free
109 functional studies via reconstitution into chemically defined liposomes.

110 111 **PROTOCOL:**

112
113 NOTE: All codon-optimized RESOLUTE SLC genes have been deposited into AddGene⁴³, the links
114 to which are available on the list of RESOLUTE public reagents⁴⁴. These genes have been cloned
115 into the pDONR221 plasmid and allow direct cloning of the genes into the destination vector
116 using recombination cloning⁴⁵. To maximize parallelism, bacterial, insect, and mammalian cells
117 are grown in block format for bacmid production (section 3), baculovirus amplification (section
118 5), and expression testing (section 6), respectively. For these steps, a micro-expression shaker is
119 required at these steps to ensure sufficient mixing and aeration.

120 121 **1. (High-throughput) cloning of SLCs into pHTBV1.1 bacmid**

122
123 NOTE: The cloning step uses a recombination cloning protocol for efficient cloning and
124 transformation into *Escherichia coli* (*E. coli*) using the heat-shock method⁴⁶. The protocol is
125 designed for high-throughput and parallel cloning of multiple targets or constructs but can be
126 readily adapted to smaller scales.

127
128 1.1. In a 96-well plate, add 150 ng of the pDONR221 SLC clone and 100 ng of the pHTBV1.1-
129 C3CGFP-SIII-10H-GTW vector. Bring the reaction volume to 8 μ L with 10 mM Tris 8.0, and then
130 add 2 μ L recombination enzyme mix.

131
132 1.2. Incubate at room temperature for 1 h, add 1 μ L of Proteinase K, and incubate for 30 min at

133 37 °C.

134

135 1.3. Use 4 µL of the reaction mixture to transform 50 µL of chemically competent *E. coli* MACH-1
136 cells using the heat-shock method ⁴⁶ and SOC medium for recovery. Plate onto LB-agar containing
137 5% sucrose, or SOC agar, supplemented with 100 µg/mL ampicillin.

138

139 1.4. Identify colonies harboring the pHTBV1.1 vector with the **SLC** gene insert using appropriate
140 primers (see **Table 1**) and standard protocols for colony PCR ⁴⁷.

141

142 1.5. Purify the recombinant plasmid from single colonies with the gene of interest using a plasmid
143 miniprep kit.

144

145 **1. Transposition**

146

147 NOTE: The following steps are used to transpose the SLC genes from the pHTBV1.1 vector into a
148 bacmid for BacMam baculovirus generation in Sf9 cells. Using the heat-shock method ⁴⁶, the
149 pHTBV1.1 vector is transformed into DH10Bac competent *E. coli* cells, which contain a parent
150 bacmid with a lacZ-mini-attTn7 fusion. Transposition occurs between the elements of the
151 pHTBV1.1 vector and the parent bacmid in the presence of the transposition proteins provided
152 by a helper plasmid ⁴⁸. See **Table 2** for the composition of solutions used in this protocol.

153

154 2.1. Using 3µL of 100–200 ng/µL purified pHTBV1.1 vector DNA, transform DH10Bac using the
155 heat-shock method in a 96-well PCR plate. Recover the cells by incubating them in recovery
156 medium for 4–5 h at 37 °C while shaking at 700 rpm in a micro-expression shaker.

157

158 2.2. Spread 50 µL of transformed cells onto DH10Bac selection plates. Incubate the plates at 37
159 °C for 48 h covered with foil.

160

161 2.3. Pick a single white colony (containing the recombinant DNA) and streak to dilution. Incubate
162 at 37 °C overnight.

163

164 **2. High-throughput bacmid production**

165

166 NOTE: The protocol describes the steps for extracting bacmids using a 96-well bacmid purification
167 kit.

168

169 3.1. Inoculate individual white colonies (isolated from the streaked to dilution plates) into wells
170 of a 96-deep-well block, containing 1 mL of 2x LB medium (**Table 2**).

171

172 2.2. Cover with a porous seal and incubate at 37 °C overnight at 700 rpm in a micro-expression
173 shaker.

174

175 3.3. Prepare a glycerol stock of the cells by mixing 120 µL of the culture with 30 µL of 60% glycerol
176 in a microtiter plate and storing at -80 °C.

177
178 2.3. Centrifuge the deep well block at $2,600 \times g$ for 30 min. Decant the supernatant into a
179 suitable container for decontamination. Invert the block and tap gently on a paper towel. Add
180 250 μL of Solution 1 to each well of the block using a multi-channel pipette.
181
182 3.5. Resuspend the pellets; if necessary, use a multi-channel pipette.
183
184 3.6. Add 250 μL of Solution 2 to each well and seal with a silicone mat. Invert gently 5x and
185 incubate at room temperature for 10 min. Spin very briefly.
186
187 3.7. Add 300 μL of Solution 3 and seal with a silicone mat. Mix gently but thoroughly by inverting
188 5x.
189
190 3.8. Place the sample on ice for 20 min, then centrifuge at $2,600 \times g$ for 30 min at 4°C .
191
192 3.9. Transfer the clear supernatant to a fresh 96-well block. Centrifuge again at $2,600 \times g$ for 30
193 min at 4°C .
194
195 3.10. In a fresh 96-deep-well block, dispense 0.8 mL of 100% isopropanol per well. Add 0.8 mL of
196 supernatants from the corresponding wells.
197
198 3.11. Gently pipette up and down using a pipette, then incubate on ice for 30 min or overnight
199 at 4°C to yield more bacmid.
200
201 3.12. Centrifuge at $2,600 \times g$ for 30 min at 4°C .
202
203 3.13. Inside a biological safety cabinet, spray the outside of the block with 70% ethanol, open the
204 block, and discard the supernatant.
205
206 3.14. Add 500 μL of 70% ethanol (v/v) to each well and tap the block gently to wash the pellet.
207 Cover with an adhesive plastic seal and centrifuge at $2,600 \times g$ for 30 min at 4°C .
208
209 3.15. Inside a Biological Safety Cabinet, open the block and discard the supernatant. Tap the block
210 very gently on a paper towel to remove the ethanol. Allow the block to dry either inside the hood
211 for 1–2 h or in a 50°C oven.
212
213 3.16. Add 50 μL of sterile TE buffer to resuspend the bacmid DNA and then, seal using a adhesive
214 plastic seal. Transfer the contents to a V-bottom microtiter plate. Store the bacmid DNA at 4°C
215 until the test purification is complete and store it at -20°C .
216
217 NOTE: While not routinely measured, generally a yield of 500 to 2,000 ng/ μL bacmid DNA can be
218 expected.
219
220 3.17. Use standard colony PCR methods⁴⁷, and the following vector primers to screen for bacmids

221 successfully incorporating the target gene:
222 pFBM-fwd caaaatgctcgtacaactccgc
223 pFBM-rev tagttaagaataaccagtcaatctttcac

224

225 NOTE: The amplicon will be approximately 700 bp bigger than the target gene.

226

227 **3. Transfection**

228

229 NOTE: These steps are used to transfect Sf9 insect cells with the bacmid produced, which causes
230 the insect cell to generate baculovirus particles (P0).

231

232 4.1. Grow Sf9 cells in serum-free insect medium to a density of $2.0\text{--}2.4 \times 10^6$ cells/mL. Dilute the
233 cells to 2×10^5 cells/mL in serum-free insect medium and dispense 1 mL of the diluted cells into
234 a 24-well tissue culture plate well. Include a *transfection-reagent-only* as well as a *cells-only*
235 control. Incubate the plate in a humidified incubator at 27 °C for 1 h to allow cell attachment.

236

237 4.2. Mix 38 μL per well of serum-free insect medium with 2 μL per well of the transfection
238 reagent. Dispense 40 μL of the mixture into a 96-well sterile flat-bottom microtiter plate. Add 2
239 μL of recombinant bacmid DNA at 0.5–2.0 $\mu\text{g}/\mu\text{L}$, cover the plate, and incubate inside the
240 microbiological safety cabinet for 15 min.

241

242 4.3. Add 160 μL of serum-free insect medium into each well of the microtiter plate containing
243 the DNA-transfection reagent mixture.

244

245 4.4. Aspirate medium from the cells in step 4.1. Gently, add the 200 μL of bacmid-transfection
246 reagent-medium mixture onto the cells, cover the plate, and incubate for 4 h in a humidified
247 incubator at 27 °C.

248

249 4.5. Add 400 μL of serum-free insect medium supplemented with 2% FBS to each well. To reduce
250 evaporation, transfer the plate into a clean plastic bag but do not seal it. Incubate the plate at 27
251 °C for 72 h in a humidified incubator.

252

253 4.6. After 3 days, transfer the media from the plate into a sterile 96-deep-well block and
254 centrifuge at $1,500 \times g$ for 20 min at room temperature. Transfer the clarified supernatant
255 containing P0 baculovirus into a sterile 96-deep-well block and store at 4 °C away from light.

256

257 **4. BacMam baculovirus amplification**

258

259 NOTE: The following steps are used to amplify the initial P0 baculovirus to higher titer viral stocks;
260 namely P1, P2, and P3. The final P3 titer is appropriate for transduction and protein expression.
261 For efficiency and parallelism, this protocol uses fixed volumetric ratios for viral amplification
262 which have been empirically optimized. However, if the transduced cells do not show GFP
263 fluorescence by microscopy and increased cell diameter, or if protein expression subsequently
264 fails (see section 8), baculovirus amplification should be re-optimized for a low multiplicity of

265 infection at each step after quantifying the baculovirus titer^{49–52}, and infection monitored by GFP
266 fluorescence microscopy and increased cell diameter⁵³.

267

268 5.1. Prepare the P1 virus stock by growing Sf9 cells in serum-free insect medium to a density of 2
269 $\times 10^6$ cells/mL, add 2% FBS, and seed the cells in a 24-deep-well block in a final volume of 3 mL
270 per well. Add 120 μ L of P0 virus stock to the cells.

271

272 5.2. Incubate the block at 27 °C while shaking at 450 rpm in a micro-expression shaker for 66–72
273 h. Centrifuge the block at $1,500 \times g$ for 20 min at room temperature and harvest the supernatant
274 into 96-deep-well blocks. Store as P1 virus stock at 4 °C away from light.

275

276 5.3. Prepare P2 virus stock by infecting 50 mL of Sf9 cells (2×10^6 cells/mL cell density), grown in
277 serum-free insect medium supplemented with 2% FBS, with 250 μ L of P1 virus stock. Incubate
278 the cells at 27 °C with shaking at 110 rpm.

279

280 5.4. Harvest P2 virus stock after 66–72 h by centrifugation at $1,500 \times g$ for 20 min and store at 4
281 °C away from light.

282

283 5.5. Prepare P3 virus stock by infecting the desired volume of Sf9 cells (2×10^6 cells/mL cell
284 density) with 1:200 (v/v) P2 viral stock. Incubate the cells at 27 °C with shaking at 110 rpm.

285

286 5.6. After 66–72 h, centrifuge at $1,500 \times g$ for 20 min and harvest the P3 virus by collecting the
287 supernatant and store at 4 °C, protected from light.

288

289 **5. Transduction for expression testing**

290

291 NOTE: The following section describes small-scale expression testing and can be modified for
292 parallel testing of multiple constructs using deep well blocks.

293

294 6.1. Prepare a 20% (w/v) polyethylene glycol solution by dissolving 200 g of PEG 10,000 and 12 g
295 of NaCl in 600 mL of double-distilled H₂O. Stir and bring to a final volume of 1,000 mL. Autoclave
296 the solution.

297

298 6.2. Add 300 μ L of harvested P1 virus into the wells of a 24-deep-well block and add 75 μ L of the
299 PEG solution to each well. Incubate the block in a micro-expression shaker at 18 °C while shaking
300 at 300 rpm for 5 min and store the block at 4 °C overnight.

301

302 6.3. Shake the block again at 300 rpm for 30 min at 18 °C and centrifuge the block at $3,000 \times g$
303 for 45 min. Discard the supernatant using a pipette in a microbiological safety cabinet.

304

305 6.4. Prepare suspension-adapted HEK293 cells in HEK293 medium, supplemented with 5 mM
306 sodium butyrate, to a density of 2×10^6 cells/mL, and seed 3 mL into each well containing the
307 virus pellet.

308

309 6.5. Incubate the block at 30 °C with 8% CO₂ while shaking at 200–250 rpm for 72 h.

310

311 NOTE: The vendor-recommended CO₂ concentrations during cell culture are different for
312 suspension-adapted and ancestral HEK293 cell lines, at 8% and 5% respectively.

313

314 6.6. Harvest the cells by centrifugation at 900 × *g* for 20 minutes and wash each well with 1 mL
315 of PBS.

316

317 NOTE: Aspirate 10 μL of resuspended cells and view the cells under a fluorescence microscope
318 with a GFP-compatible filter cube to assess protein expression and localization. Aspirate 10–15
319 μL of resuspended cells and run a whole-cell SDS-PAGE gel for in-gel green fluorescent protein
320 (GFP) fluorescence detection 54.

321

322 6.7. Centrifuge again at 900 × *g* for 20 min. Freeze the pellets at –80 °C.

323

324 6. High-throughput small-scale test purification

325

326 NOTE: The following steps describe a rapid test purification workflow in a 24-well block format
327 for screening the expression levels of individual SLCs. See **Table 2** for the composition of solutions
328 used in this protocol.

329

330 7.1. Add 1 mL of HT lysis buffer to each well of harvested cells and proceed to sonicate on ice for
331 a total length of 4 min (3 s on/15 s off) in 24-well blocks using a 24-head probe.

332

333 7.2. Transfer the contents to a 96-deep well block, add 125 μL of detergent stock, and seal with
334 a silicon seal. Rotate the block gently at 4 °C for 1 h. Alternatively, add dodecylmaltoside (DDM)
335 and cholesterol hemisuccinate (CHS) directly to the 24-well blocks and place them on a rocker-
336 shaker at 4 °C.

337

338 7.3. Centrifuge the block at 2600 × *g* for 20 min at 4 °C and transfer the supernatant into a new
339 96-deep-well block.

340

341 7.4. Prepare a 50% stock of high-capacity resin preequilibrated with lysis buffer.

342

343 7.5. Add 100 μL of resuspended resin stock to each well.

344

345 7.6. Cover the block with a silicon seal and rotate at 4 °C for 2 h and then, centrifuge very briefly
346 (up to 200 × *g* and back down) to remove liquid sticking to the cover.

347

348 7.7. Place a 96-well filter plate on top of an empty block and transfer the resin/supernatant mix
349 into the filter plate. Rinse out the wells of the deep well block with 800 μL of HT wash buffer and
350 transfer to the filter block to collect the maximum amount of resin.

351

352 7.8. Allow the buffer to drip through or centrifuge briefly at 200 × *g* and collect the flowthrough.

353 Place the filter plate on top of a new wash block and wash the resin with 800 μ L of HT wash
354 buffer, allowing the buffer to drip through (or centrifuge briefly). Repeat the wash step two more
355 times and centrifuge the block at 500 $\times g$ for 3 min to remove the residual HT wash buffer.

356

357 7.9. Place the filter plate on top of a 96-well microtiter plate. Add 50 μ L of HT elution buffer and
358 incubate with shaking at room temperature for 10 min. Elute samples by centrifuging at 500 $\times g$
359 for 3 min.

360

361 7.10. Run 15 μ L of the eluted sample on a Coomassie-stained SDS-PAGE gel to check the protein
362 expression. Load the remaining samples of eluent onto a Size Exclusion Chromatography (SEC) or
363 Fluorescence-detection Size Exclusion Chromatography (FSEC) system to evaluate protein
364 monodispersity in DDM/CHS.

365

366 7. Transduction for large-scale expression

367

368 NOTE: The following steps are the standard RESOLUTE protocol for SLC expression. Individual
369 targets will require further optimization for the expression length, incubation temperature, and
370 concentration of sodium butyrate. Further, we routinely optimize the baculovirus multiplicity of
371 infection by testing various volumetric ratios of the P3 virus used to infect the suspension-
372 adapted HEK293 cells in small-scale experiments. This is time efficient, uses techniques and
373 equipment already at hand, and directly evaluates the desired experimental output. However,
374 this empirical method requires re-optimization with each amplification of the P3 virus, and other
375 methods are available to quantify the baculovirus particles^{49–52}.

376

377 8.1. Scale up the required volume of suspension-adapted HEK293 cells in HEK293 medium.

378

379 8.2. Dilute suspension-adapted HEK293 cells to 1 $\times 10^6$ cells/mL and grow for 24 h (at 170 rpm
380 for 2 L roller bottles and 105 rpm for 3 L roller bottles).

381

382 8.3. Add 30 mL of P3 virus per liter of cells and add 5 mM sodium butyrate. Incubate cells at 37
383 $^{\circ}$ C for 48 h or at 30 $^{\circ}$ C for 72 h.

384

385 8.4. During and after the incubation period, a **Key Step** is to examine the cells using brightfield
386 microscopy to check for microbial contamination and cell viability. Assess protein expression and
387 localization using fluorescence microscopy with a GFP-compatible filter cube.

388

389 8.5. Harvest the cells by centrifugation at 900 $\times g$ for 20 min.

390

391 8.6. Wash the cell pellet by resuspending it in 10–15 mL of PBS per liter of cell culture and pellet
392 again at 900 $\times g$ for 20 min.

393

394 8.7. Snap-freeze the cell pellets in liquid nitrogen and store them at -80 $^{\circ}$ C.

395

396 9. Protein purification

397 NOTE: The following is the standard RESOLUTE method for SLC purification for 5 L of cell culture.
398 For each SLC target, the optimal detergent must be determined empirically. Prepare base buffer,
399 detergent stock solution, wash, elution, and SEC buffers in advance (**Table 2**). For a list of the
400 standard detergents tested, see **Table 3**. ATP and MgCl₂ in the wash buffer reduce contamination
401 by heat-shock proteins.

402

403 **9.1. Day 1**

404

405 9.1.1. Thaw the frozen cell pellet in a water bath set to room temperature.

406

407 9.1.2. Prepare solubilization buffer with 135 mL of base buffer and three protease Inhibitor
408 Cocktail tablets. Allow the tablets to dissolve.

409

410 9.1.3. Suspend the thawed pellet with solubilization buffer. Use 27 mL of solubilization buffer per
411 10–15 g of cell pellet, add DNase, and pour into an ice-cold Dounce homogenizer. Homogenize
412 the solution by moving the plunger up and down approximately 20x, keeping the homogenizer
413 on ice.

414

415 NOTE: The resuspension volume will need to be optimized based on the target protein and the
416 cell pellet mass, which will vary due to the cell density at harvest. Commercial DNase can be
417 added as per the manufacturer's instructions. DNase can also be expressed and purified in-house
418 using established protocols⁵⁵.

419

420 9.1.4 Add detergent stock solution to 1% final concentration.

421

422 NOTE: A **Key Step** to optimizing protein purification is identifying the optimal detergent for SLC
423 solubilization and purification, which must be identified empirically. We have regularly utilized
424 various detergents; each alone and in combination with cholesteryl hemisuccinate, keeping the
425 detergent to CHS mass ratio at 10:1.

426

427 9.1.5. Transfer the solubilization mixture to 50 mL conical tubes. Rotate slowly for 1 h at 4 °C.

428

429 9.1.6. Centrifuge the solution at 50,000 × *g* for 30 min at 4 °C. Collect the supernatant.

430

431 9.1.7. Equilibrate 4–6 mL bed volume of Strep-Tactin resin with the base buffer.

432

433 9.1.8. Add equilibrated resin to the solubilized supernatant and rotate for 2 h at 4 °C.

434

435 9.1.9. Pour the solution into a gravity flow column and allow the solution to flow through.

436

437 9.1.10. Wash the resin with 30X the bed volume of Strep wash buffer in 3 equal steps.

438

439 9.1.11. Add 3–5 mL of elution buffer, incubate for 15 min, and collect the eluate. Repeat this step
440 four more times, collecting each elution fraction separately.

441

442 NOTE: A **Key Step** is protein elution from the Strep-Tactin resin, where it is important to incubate
443 for 15 min after each addition of the elution buffer. Typically, the first eluate fraction contains a
444 lower concentration of protein due to the dilution of the elution buffer by the residual wash
445 buffer. Therefore, the first eluate fraction may be discarded if a higher final protein concentration
446 is desired. Alternatively, the protein concentration in all serial elutions may also be analyzed using
447 SDS-PAGE to optimize the protocol.

448

449 9.1.12. Measure protein concentration by UV absorbance spectroscopy, combine the desired
450 elution fractions, and add 3C protease at the ratio of 1:5 (w/w) to 1:10 (w/w).

451

452 9.1.13. Rotate slowly overnight at 4 °C.

453

454 NOTE: Steps 9.1.12 and 9.1.13 is only necessary if the GFP tag needs removal. If the tag removal
455 is not required, proceed to Step 9.2.4 directly. Alternatively, the protein can be kept at 4 °C
456 overnight to continue the following day. Furthermore, for SLCs with diminished stability, the
457 protease concentration, incubation period, and temperature may need optimization. The 3C
458 protease is active over a wide range of temperatures and allows for optimization best suited for
459 various SLCs.

460

461 9.2.1 Day 2

462

463 9.2.1. Equilibrate 2–4 mL of bed volume of cobalt metal affinity resin with SEC buffer.

464

465 9.2.2. Add equilibrated cobalt metal affinity resin to the overnight 3C reaction mixture and rotate
466 for 1 h at 4 °C.

467

468 9.2.3. Pour the solution into a gravity flow column and collect the flowthrough.

469

470 9.2.4. Concentrate the flowthrough in a 100 kDa cut-off centrifugal filter by spinning at 3,000 × *g*
471 at 4 °C and gently mix the sample every 5 min until the desired SEC injection volume is reached.

472

473 9.2.5. Equilibrate a dextran-agarose-based size exclusion chromatography column using SEC
474 buffer. The SEC procedure should be carried out at 4 °C (cooled chamber or cold room).

475

476 NOTE: **Key step:** Depending on the oligomeric state of the SLC, a different column, such as an
477 agarose-based size exclusion chromatography column, may be used to perform SEC.

478

479 9.2.6. Inject the sample into the sample loop and run the SEC program, with a flow rate such that
480 column pressure is below the column manufacturer's specifications. Using a fraction collector,
481 automatically collect 0.3mL fractions over the entire SEC run.

482

483 9.2.7. Pool peak fractions, measure UV absorbance at 280 nm, and concentrate in a 100 kDa cut-
484 off centrifugal concentrator to the required volume/concentration by spinning at 3,000 × *g* at 4

485 °C.

486

487 **REPRESENTATIVE RESULTS:**

488 **SLC genes can be cloned from RESOLUTE pDONR plasmids into BacMam vectors for mammalian** 489 **expression**

490 The described protocols for cloning, expression, and purification have proven successful for many
491 SLC transporters across multiple protein folds. Nevertheless, the procedures include several
492 checkpoints for monitoring progress, allowing for optimization to account for differences in
493 expression, protein folding, lipid- and detergent-dependent stability, and sensitivity to buffer
494 conditions.

495

496 **Checkpoints during SLC cloning and small-scale expression**

497 In the cloning steps, agarose gel electrophoresis should be used to ensure the correct size of the
498 PCR and digestion products. Similarly, the Gateway and transposition reactions can be validated
499 with a colony PCR reaction (**Figure 2A,B**). Baculovirus generation can be monitored using as
500 necessary^{49–52}. The initial expression should be done at a small scale, evaluating protein yield by
501 SDS-PAGE (**Figure 2B**). Similarly, the fraction of green fluorescent cells, total protein expression,
502 and protein localization should be noted using fluorescence microscopy (**Figure 2C,D**). Protein
503 expression should be optimized for cell type, temperature, time, and the necessity of chaperones
504 and complex partners. The expression can be further optimized by modifying the construct to
505 truncate disordered N- and C-termini, based on secondary structure prediction^{56–58}, and testing
506 the types and placement of affinity tags. Protein stability should be evaluated at a small scale by
507 FSEC (**Figure 2E**), SEC-based thermal shift assay (SEC-Ts), and DSF^{41,42,59–62}. Small molecules, such
508 as substrates and inhibitors, detergents, cholesterol hemisuccinate, lipids, and pH should be
509 tested for improving protein stability considering the protein's function and native subcellular
510 environment and subsequent purification buffers modified accordingly. In both small- and large-
511 scale expression setups, cells should be monitored using microscopy for viability and
512 contamination.

513

514 **Optimization of transporter purification at large scale**

515 Each step of large-scale protein purification should be evaluated by SDS-PAGE, including in-gel
516 fluorescence to specifically monitor the GFP-tagged protein and enzymatic removal of that tag.
517 In practice, the GFP-tagged SLC-expressing cells appear yellowish-green. After Twin-Strep-tag
518 chromatographic elution, the eluent containing the purified protein appears fluorescent neon-
519 green under white light. Chemically and structurally homogeneous protein should yield a single
520 monodisperse A₂₈₀ peak during size-exclusion chromatography (**Figure 2F,G**), and should show a
521 single band on SDS-PAGE. The SDS-PAGE band corresponding to the expected SLC, and any
522 unexpected bands, should be analyzed using tryptic digestion mass-spectrometry. Multiple
523 bands on the SDS-PAGE gel indicate either proteolytic degradation, contaminating proteins, or
524 SDS-resistant oligomers. Contaminating proteins may be removed by increasing the NaCl
525 concentration of the solubilization buffer or changing the affinity tag. Proteolysis can be limited
526 by improving the protein's purity, ensuring all steps are done at 4 °C or on ice, and optimizing the
527 protocol to minimize the time of each step. If the SEC profile has a broad peak, multiple peaks,
528 or large void peak (such as the purple trace of **Figure 2E**), the construct and purification

529 conditions should be optimized at a small scale using FSEC, SEC-Ts, or DSF ^{41, 42, 59–62}.

530

531 **FIGURE AND TABLE LEGENDS:**

532 **Figure 1: Schematic of RESOLUTE workflow for SLC expression and purification.** Step-by-step
533 illustration of recombination cloning, BacMam baculovirus preparation, protein expression and
534 purification, and downstream applications. Abbreviations: SLC = solute carrier; Cryo-EM = cryo-
535 electron microscopy; SEC = size exclusion chromatography.

536

537 **Figure 2: Representative results for SLC expression and purification.** (A) Colony PCR of high-
538 throughput SLC cloning into pHTBV1.1-C3CGFP-SIII-10H-GTW. (B) Coomassie-stained SDS-PAGE
539 of single small-scale, parallel expression test of 24 different full-length SLCs. (C) In-cell
540 fluorescence of a GFP-tagged SLC localizing primarily to the plasma membrane. (D) In-cell
541 fluorescence of a GFP-tagged SLC with significant intracellular localization. (E) Representative
542 FSEC traces for four SLCs resolved on a hydrophilic, neutral silica-based UHPLC column.
543 Representative SEC traces for six SLCs purified on either a (F) dextran-agarose or (G) agarose size
544 exclusion chromatography columns. Molecular weights of the SLC complex and detergent used
545 for purification are indicated where the oligomeric state has been experimentally determined.
546 Abbreviations: SLC = solute carrier; GFP = green fluorescent protein; FSEC = fluorescence-
547 detection size exclusion chromatography.

548

549 **Figure 3: Downstream applications of purified SLCs.** (A) Micrograph of SLC1A1 in detergent. (B)
550 2D class averages of SLC1A1 in detergent. (C) Raw fluorescence of CPM thermal denaturation
551 assay of SLC10A6 incubated with various concentrations of Tauroolithocholic acid 3-sulfate. (D)
552 First derivative of CPM thermal denaturation of SLC10A6. The SLC10A6's melting temperature
553 increased by 10 °C in the presence of 120 μM Tauroolithocholic acid 3-sulfate. Abbreviations: SLC
554 = solute carrier; CPM = *N*-[4-(7-diethylamino-4-methyl-3-coumarinyl)phenyl]maleimide.

555

556 **Table 1: Plasmids used for RESOLUTE cloning and BacMam generation.**

557

558 **Table 2: A list of solutions used in this protocol and their composition.**

559

560 **Table 3: Standard detergents used to test membrane solubilization and SLC monodispersity
561 and stability.**

562

563 **DISCUSSION:**

564 The development of SLC-targeting therapies has remained hampered due to the absence of
565 systematic characterization of transporter function. This has led to disproportionately fewer drugs
566 targeting this protein class relative to GPCRs and ion channels ⁶³, despite their numerous roles in
567 normal and pathophysiological processes. RESOLUTE is an international consortium aimed at
568 developing cutting-edge research techniques and tools to accelerate and improve current SLC
569 research. As a part of RESOLUTE, we have developed these protocols for efficient cloning,
570 construct screening, and large-scale expression and purification of human SLCs.

571

572 Here we describe scalable SLC cloning and expression methods that were successfully used to

573 systematically explore the human SLC transporters, including putative and orphan SLCs. Notably,
574 SLCs purified in this manner have been successfully used in subsequent studies of transporter
575 structure, biochemistry, function, binder generation, and small-molecule binding. We regularly
576 employ this method to purify milligram quantities of various SLCs and under optimal conditions,
577 the entire protocol, including the cloning and tissue culture steps, can be completed in 4–5
578 weeks.

579
580 Our method is optimized for economy and parallelism to systematically evaluate multiple targets.
581 However, this high-throughput method is also readily adapted to the parallel generation of
582 constructs for a single target with distinct truncations or tags by using distinct cloning primers or
583 vectors. This is similar methods also optimize multiple constructs for a target ⁶⁴, though our
584 protocol offers further efficiencies with parallel cloning, baculovirus generation, and expression
585 testing. Transfection offers a shorter time between construct cloning and expression by forgoing
586 the baculovirus generation ⁶⁵ but is significantly more expensive and laborious for large-scale
587 expression. In contrast, stable cell lines are likely less expensive for large-scale expression ⁶⁶, but
588 generating highly-expressing clonal cell lines can require more time and specialized resources.
589 Finally, while this protocol uses human cell lines for protein production, insect cells line such as
590 from *Spodoptera frugiperda* and *Trichoplusia ni* have also been successfully used for large-scale
591 SLC expression ^{5, 31, 64}. Expression in human cell lines increases media costs but offers more
592 native-like post-translation modifications and lipid environment ^{39, 67}.

593
594 While the protocol can be adapted for different membrane transporters and experimental needs,
595 several factors influence the quality and yield of the purified protein samples. While it is ideal to
596 study full-length proteins, some degree of sequence truncation may be required to achieve
597 better expression/reconstitution and purification yield. All Resolute SLC constructs have been
598 tagged with a cleavable GFP, which is valuable in monitoring SLC expression, cellular localization,
599 and purification. The suspension-adapted HEK293 cell expression system used in these
600 experiments has led to superior yields and is recommended, although we routinely also produce
601 proteins without complex glycosylation via the suspension-adapted HEK293 GnTI- cell line. The
602 incubation temperature and length for protein expression by transduced cells should be
603 optimized for each target, though we have found 72 h at 30 °C to be a good default.

604
605 All protein purification steps should be carried out on ice or 4 °C and once the purified protein
606 has been snap-frozen, freeze-thaw cycles should be avoided. The type and amount of the
607 detergents used in membrane solubilization and purification buffers are critical and should be
608 determined for each SLC empirically.

609
610 The SLCs purified with this method yield homogeneous and structurally and functionally intact
611 samples, which can be used for a variety of biochemical and biophysical studies. Observing single,
612 discrete particles of the solubilized and purified SLC protein by negative stain and Cryo-EM
613 (**Figure 3A,B**) can be promising for subsequent structure determination ³⁷. The purified SLC in
614 detergent can be used for biophysical assays such as thermal stability assay (**Figure 3C,D**) to
615 investigate the protein interactions with small molecules such as substrates, inhibitors, or lipids
616 ^{59, 62}. Finally, the SLCs purified using this protocol in biochemical assays can be reconstitution into

617 liposomes or nanodiscs for functional assays ⁶⁸ and used for antibody and nanobody generation
618 and selection ^{69, 70}. While it remains a challenge to adapt these methods to the throughput
619 necessary for the discovery of new SLC-targeted small molecules ¹, promising advances have
620 been made *in vivo* high-throughput screening technologies ^{71–74}.

621

622 **ACKNOWLEDGMENTS:**

623 This work was performed within the RESOLUTE project. RESOLUTE has received funding from the
624 Innovative Medicines Initiative 2 Joint Undertaking under grant agreement No 777372. This Joint
625 Undertaking receives support from the European Union's Horizon 2020 research and innovation
626 programme and EFPIA. This article reflects only the authors' views and neither IMI nor the
627 European Union and EFPIA are responsible for any use that may be made of the information
628 contained therein. The pHTBV plasmid was kindly provided by Prof. Frederick Boyce (Harvard).

629

630 **DISCLOSURES:**

631 The authors declare no competing financial interests.

632

633 **REFERENCES:**

- 634 1. Wang, W. W., Gallo, L., Jadhav, A., Hawkins, R., Parker, C. G. The druggability of solute
635 carriers. *Journal of Medicinal Chemistry*. **63** (8), 3834–3867 (2020).
- 636 2. Liao, J. et al. Structural insight into the ion-exchange mechanism of the sodium/calcium
637 exchanger. *Science*. **335** (6069), 686–690 (2012).
- 638 3. Bröer, S., Gether, U. The solute carrier 6 family of transporters: the solute carrier family
639 6. *British Journal of Pharmacology*. **167** (2), 256–278 (2012).
- 640 4. Anderson, C. M., Stahl, A. SLC27 fatty acid transport proteins. *Molecular Aspects of*
641 *Medicine*. **34** (2–3), 516–528 (2013).
- 642 5. Nguyen, L. N. et al. Mfsd2a is a transporter for the essential omega-3 fatty acid
643 docosahexaenoic acid. *Nature*. **509** (7501), 503–506 (2014).
- 644 6. Kobayashi, N. et al. MFSD2B is a sphingosine 1-phosphate transporter in erythroid cells.
645 *Scientific Reports*. **8** (1), 4969 (2018).
- 646 7. Kawahara, A. et al. The sphingolipid transporter Spns2 functions in migration of zebrafish
647 myocardial precursors. *Science*. **323** (5913), 524–527 (2009).
- 648 8. Kandasamy, P., Gyimesi, G., Kanai, Y., Hediger, M. A. Amino acid transporters revisited:
649 New views in health and disease. *Trends in Biochemical Sciences*. **43** (10), 752–789 (2018).
- 650 9. Navale, A. M., Paranjape, A. N. Glucose transporters: physiological and pathological roles.
651 *Biophysical Reviews*. **8** (1), 5–9 (2016).
- 652 10. Pajor, A. M. Molecular properties of the SLC13 family of dicarboxylate and sulfate
653 transporters. *Pflügers Archiv - European Journal of Physiology*. **451** (5), 597–605 (2006).
- 654 11. Nwosu, Z. C., Song, M. G., Di Magliano, M. P., Lyssiotis, C. A., Kim, S. E. Nutrient
655 transporters: connecting cancer metabolism to therapeutic opportunities. *Oncogene*. **42** (10),
656 711–724 (2023).
- 657 12. Girardi, E. et al. A widespread role for SLC transmembrane transporters in resistance to
658 cytotoxic drugs. *Nature Chemical Biology*. **16** (4), 469–478 (2020).
- 659 13. Nigam, S. K. The SLC22 transporter family: a paradigm for the impact of drug transporters
660 on metabolic pathways, signaling, and disease. *Annual Review of Pharmacology and Toxicology*.

661 **58** (1), 663–687 (2018).

662 14. Cheng, M. H. et al. Insights into the modulation of dopamine transporter function by
663 amphetamine, orphenadrine, and cocaine binding. *Frontiers in Neurology*. **6**, 134 (2015).

664 15. Sachkova, A., Doetsch, D. A., Jensen, O., Brockmöller, J., Ansari, S. How do
665 psychostimulants enter the human brain? Analysis of the role of the proton-organic cation
666 antiporter. *Biochemical Pharmacology*. **192**, 114751 (2021).

667 16. Lin, L., Yee, S. W., Kim, R. B., Giacomini, K. M. SLC transporters as therapeutic targets:
668 emerging opportunities. *Nature Reviews Drug Discovery*. **14** (8), 543–560 (2015).

669 17. Yernool, D., Boudker, O., Jin, Y., Gouaux, E. Structure of a glutamate transporter
670 homologue from *Pyrococcus horikoshii*. *Nature*. **431** (7010), 811–818 (2004).

671 18. Huang, Y., Lemieux, M. J., Song, J., Auer, M., Wang, D. -N. Structure and mechanism of the
672 glycerol-3-phosphate transporter from *Escherichia coli*. *Science*. **301** (5633), 616–620 (2003).

673 19. Yamashita, A., Singh, S. K., Kawate, T., Jin, Y., Gouaux, E. Crystal structure of a bacterial
674 homologue of Na⁺/Cl⁻-dependent neurotransmitter transporters. *Nature*. **437** (7056), 215–223
675 (2005).

676 20. Sauer, D. B. et al. Structural basis for the reaction cycle of DASS dicarboxylate
677 transporters. *eLife*. **9**, e61350 (2020).

678 21. Levin, E. J., Quick, M., Zhou, M. Crystal structure of a bacterial homologue of the kidney
679 urea transporter. *Nature*. **462** (7274), 757–761 (2009).

680 22. Abramson, J. et al. Structure and mechanism of the lactose permease of *Escherichia coli*.
681 *Science*. **301** (5633), 610–615 (2003).

682 23. Faham, S. et al. The crystal structure of a sodium galactose transporter reveals
683 mechanistic insights into Na⁺ /sugar symport. *Science*. **321** (5890), 810–814 (2008).

684 24. Lopez-Redondo, M. L., Coudray, N., Zhang, Z., Alexopoulos, J., Stokes, D. L. Structural basis
685 for the alternating access mechanism of the cation diffusion facilitator YiiP. *Proceedings of the*
686 *National Academy of Sciences*. **115** (12), 3042–3047 (2018).

687 25. Mulligan, C. et al. The bacterial dicarboxylate transporter VcINDY uses a two-domain
688 elevator-type mechanism. *Nature Structural & Molecular Biology*. **23** (3), 256–263 (2016).

689 26. Kermani, A. A. A guide to membrane protein X-ray crystallography. *The FEBS Journal*. **288**
690 (20), 5788–5804 (2021).

691 27. Carpenter, E. P., Beis, K., Cameron, A. D., Iwata, S. Overcoming the challenges of
692 membrane protein crystallography. *Current Opinion in Structural Biology*. **18** (5), 581–586 (2008).

693 28. Sonoda, Y. et al. Benchmarking membrane protein detergent stability for improving
694 throughput of high-resolution X-ray structures. *Structure*. **19** (1), 17–25 (2011).

695 29. Wang, H. et al. Structural basis for action by diverse antidepressants on biogenic amine
696 transporters. *Nature*. **503** (7474), 141–145 (2013).

697 30. Malinauskaite, L. et al. A mechanism for intracellular release of Na⁺ by
698 neurotransmitter/sodium symporters. *Nature Structural & Molecular Biology*. **21** (11), 1006–
699 1012 (2014).

700 31. Sauer, D. B. et al. Structure and inhibition mechanism of the human citrate transporter
701 NaCT. *Nature*. **591** (7848), 157–161 (2021).

702 32. Qiu, B., Matthies, D., Fortea, E., Yu, Z., Boudker, O. Cryo-EM structures of excitatory amino
703 acid transporter 3 visualize coupled substrate, sodium, and proton binding and transport. *Science*
704 *Advances*. **7** (10), eabf5814 (2021).

- 705 33. Canul-Tec, J. C. et al. Structure and allosteric inhibition of excitatory amino acid
706 transporter 1. *Nature*. **544** (7651), 446–451 (2017).
- 707 34. Coleman, J. A., Green, E. M., Gouaux, E. X-ray structures and mechanism of the human
708 serotonin transporter. *Nature*. **532** (7599), 334–339 (2016).
- 709 35. Han, L. et al. Structure and mechanism of the SGLT family of glucose transporters. *Nature*.
710 **601** (7892), 274–279 (2022).
- 711 36. Choy, B. C., Cater, R. J., Mancina, F., Pryor, E. E. A 10-year meta-analysis of membrane
712 protein structural biology: Detergents, membrane mimetics, and structure determination
713 techniques. *Biochimica et Biophysica Acta (BBA) - Biomembranes*. **1863** (3), 183533 (2021).
- 714 37. Piper, S. J., Johnson, R. M., Wootten, D., Sexton, P. M. Membranes under the magnetic
715 lens: a dive into the diverse world of membrane protein structures using Cryo-EM. *Chemical*
716 *Reviews*. **122** (17), 13989–14017 (2022).
- 717 38. Superti-Furga, G. et al. The RESOLUTE consortium: unlocking SLC transporters for drug
718 discovery. *Nature Reviews Drug Discovery*. **19** (7), 429–430 (2020).
- 719 39. Fornwald, J. A., Lu, Q., Boyce, F. M., Ames, R. S. Gene expression in mammalian cells using
720 BacMam, a modified baculovirus system. *Baculovirus and Insect Cell Expression Protocols*. **1350**,
721 95–116 (2016).
- 722 40. Mahajan, P. et al. Expression screening of human integral membrane proteins using
723 BacMam. *Structural Genomics*. **2199**, 95–115 (2021).
- 724 41. Kawate, T., Gouaux, E. Fluorescence-detection size-exclusion chromatography for
725 precrystallization screening of integral membrane proteins. *Structure*. **14** (4), 673–681 (2006).
- 726 42. Hattori, M., Hibbs, R. E., Gouaux, E. A fluorescence-detection size-exclusion
727 chromatography-based thermostability assay for membrane protein precrystallization screening.
728 *Structure*. **20** (8), 1293–1299 (2012).
- 729 43. Fan, M., Tsai, J., Chen, B., Fan, K., LaBaer, J. A central repository for published plasmids.
730 *Science*. **307** (5717), 1877–1877 (2005).
- 731 44. Resolute Public Reagents. <https://re-solute.eu/resources/reagents> (2023).
- 732 45. Hartley, J. L. DNA cloning using in vitro site-specific recombination. *Genome Research*. **10**
733 (11), 1788–1795 (2000).
- 734 46. Froger, A., Hall, J. E. Transformation of Plasmid DNA into *E. coli* using the heat shock
735 method. *Journal of Visualized Experiments*. (6), 253 (2007).
- 736 47. Bergkessel, M., Guthrie, C. Colony PCR. *Methods in Enzymology*. **529**, 299–309 (2013).
- 737 48. Luckow, V. A., Lee, S. C., Barry, G. F., Olins, P. O. Efficient generation of infectious
738 recombinant baculoviruses by site-specific transposon-mediated insertion of foreign genes into
739 a baculovirus genome propagated in *Escherichia coli*. *Journal of Virology*. **67** (8), 4566–4579
740 (1993).
- 741 49. Dulbecco, R., Vogt, M. Some problems of animal virology as studied by the Plaque
742 Technique. *Cold Spring Harbor Symposia on Quantitative Biology*. **18** (0), 273–279 (1953).
- 743 50. Hitchman, R. B., Siaterli, E. A., Nixon, C. P., King, L. A. Quantitative real-time PCR for rapid
744 and accurate titration of recombinant baculovirus particles. *Biotechnology and Bioengineering*.
745 **96** (4), 810–814 (2007).
- 746 51. Hopkins, R. F., Esposito, D. A rapid method for titrating baculovirus stocks using the Sf-9
747 Easy Titer cell line. *BioTechniques*. **47** (3), 785–788 (2009).
- 748 52. Shen, C. F., Meghrou, J., Kamen, A. Quantitation of baculovirus particles by flow

749 cytometry. *Journal of Virological Methods*. **105** (2), 321–330 (2002).

750 53. Janakiraman, V., Forrest, W. F., Seshagiri, S. Estimation of baculovirus titer based on viable
751 cell size. *Nature Protocols*. **1** (5), 2271–2276 (2006).

752 54. Bird, L. E. et al. Green fluorescent protein-based expression screening of membrane
753 proteins in *Escherichia coli*. *Journal of Visualized Experiments*. (95), 52357 (2015).

754 55. Biedermann, K., Jepsen, P. K., Riise, E., Svendsen, I. Purification and characterization of a
755 *Serratia marcescens* nuclease produced by *Escherichia coli*. *Carlsberg Research Communications*.
756 **54** (1), 17–27 (1989).

757 56. Cong, Q., Grishin, N. V. MESSA: MEta-Server for protein Sequence Analysis. *BMC Biology*.
758 **10** (1), 82 (2012).

759 57. Jumper, J. et al. Highly accurate protein structure prediction with AlphaFold. *Nature*. **596**
760 (7873), 583–589 (2021).

761 58. Baek, M. et al. Accurate prediction of protein structures and interactions using a three-
762 track neural network. *Science*. **373** (6557), 871–876 (2021).

763 59. Mancusso, R., Karpowich, N. K., Czyzewski, B. K., Wang, D. -N. Simple screening method
764 for improving membrane protein thermostability. *Methods*. **55** (4), 324–329 (2011).

765 60. Majd, H. et al. Screening of candidate substrates and coupling ions of transporters by
766 thermostability shift assays. *eLife*. **7**, e38821 (2018).

767 61. Nji, E., Chatzikyriakidou, Y., Landreh, M., Drew, D. An engineered thermal-shift screen
768 reveals specific lipid preferences of eukaryotic and prokaryotic membrane proteins. *Nature*
769 *Communications*. **9** (1), 4253 (2018).

770 62. Alexandrov, A. I., Mileni, M., Chien, E. Y. T., Hanson, M. A., Stevens, R. C. Microscale
771 fluorescent thermal stability assay for membrane proteins. *Structure*. **16** (3), 351–359 (2008).

772 63. Santos, R. et al. A comprehensive map of molecular drug targets. *Nature Reviews Drug*
773 *Discovery*. **16** (1), 19–34 (2017).

774 64. Goehring, A. et al. Screening and large-scale expression of membrane proteins in
775 mammalian cells for structural studies. *Nature Protocols*. **9** (11), 2574–2585 (2014).

776 65. Kaipa, J. M., Krasnoselska, G., Owens, R. J., Van Den Heuvel, J. Screening of membrane
777 protein production by comparison of transient expression in insect and mammalian cells.
778 *Biomolecules*. **13** (5), 817 (2023).

779 66. Khanppnavar, B. et al. Structural basis of organic cation transporter-3 inhibition. *Nature*
780 *Communications*. **13** (1), 6714 (2022).

781 67. Marheineke, K., Grünewald, S., Christie, W., Reiländer, H. Lipid composition of *Spodoptera*
782 *frugiperda* (Sf9) and *Trichoplusia ni* (Tn) insect cells used for baculovirus infection. *FEBS Letters*.
783 **441** (1), 49–52 (1998).

784 68. Majeed, S., Ahmad, A. B., Sehar, U., Georgieva, E. R. Lipid membrane mimetics in
785 functional and structural studies of integral membrane proteins. *Membranes*. **11** (9), 685 (2021).

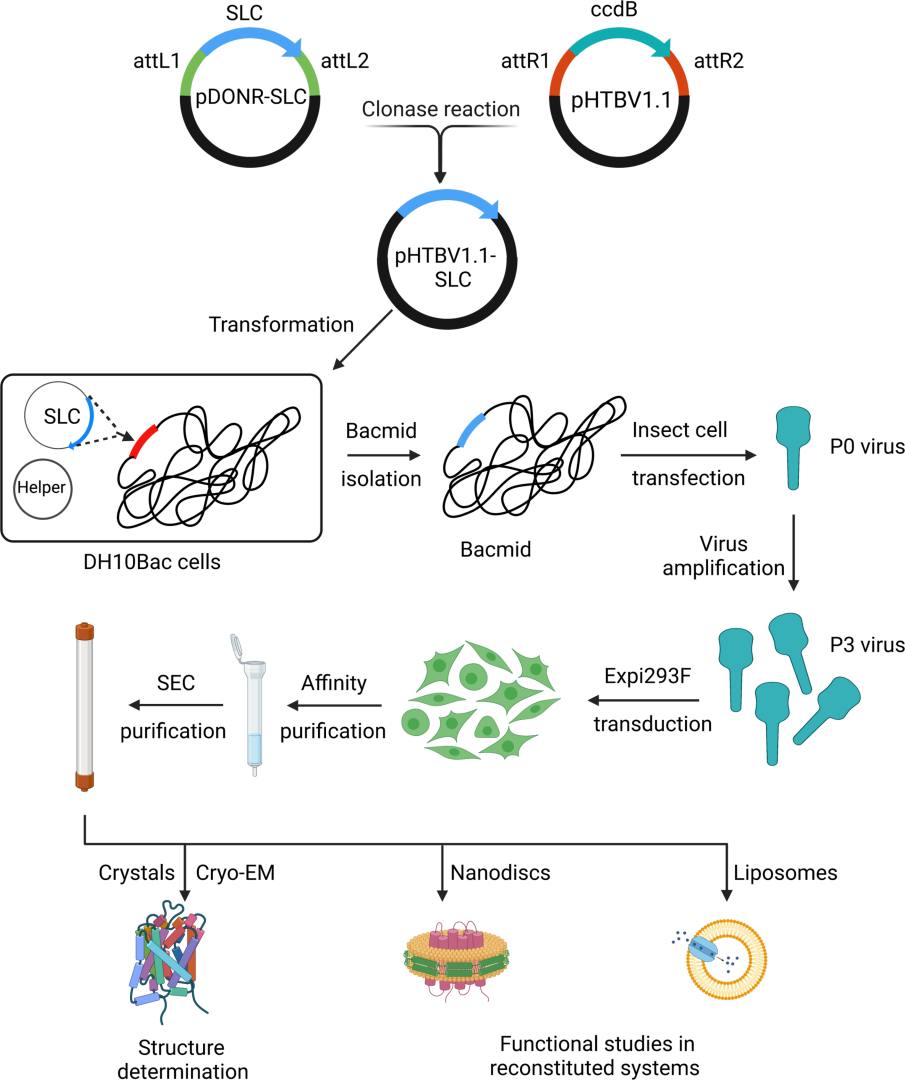
786 69. Schenck, S. et al. Generation and characterization of anti-VGLUT nanobodies acting as
787 inhibitors of transport. *Biochemistry*. **56** (30), 3962–3971 (2017).

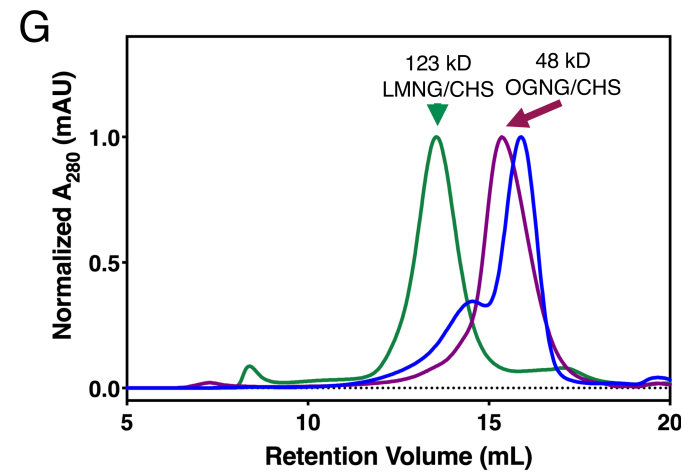
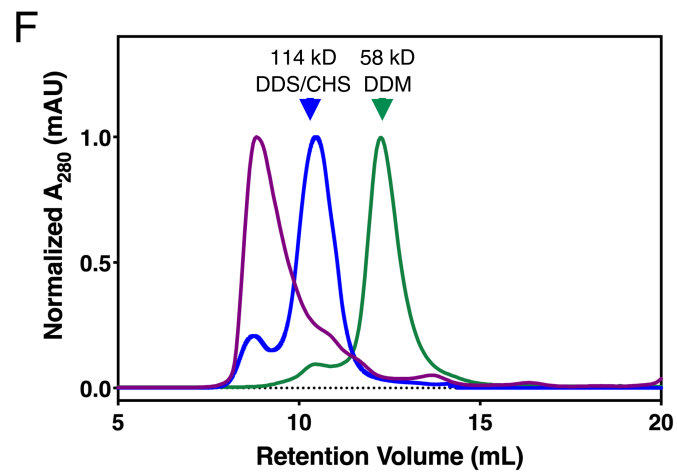
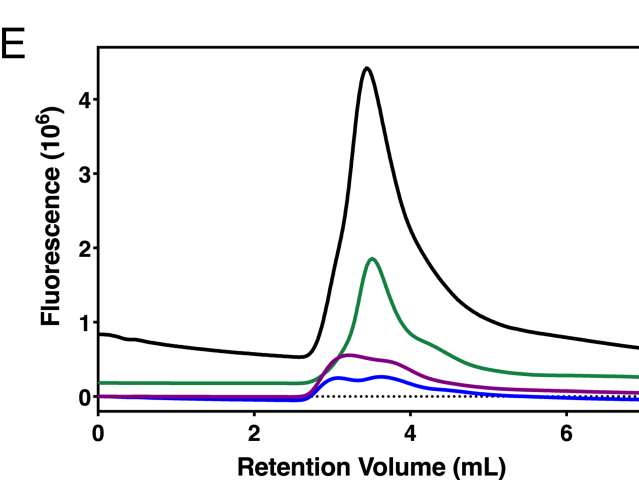
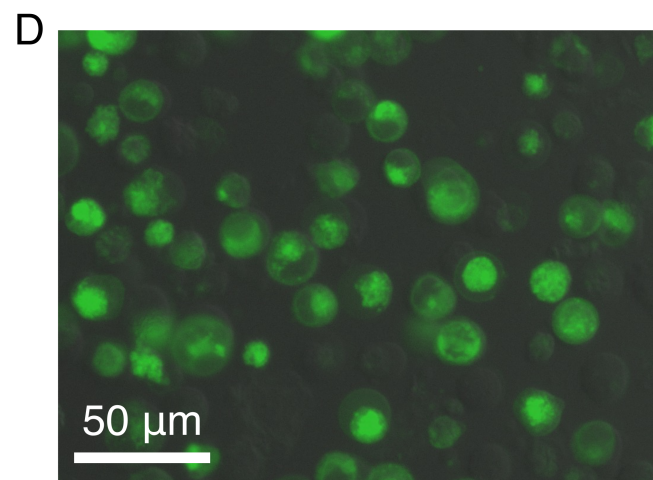
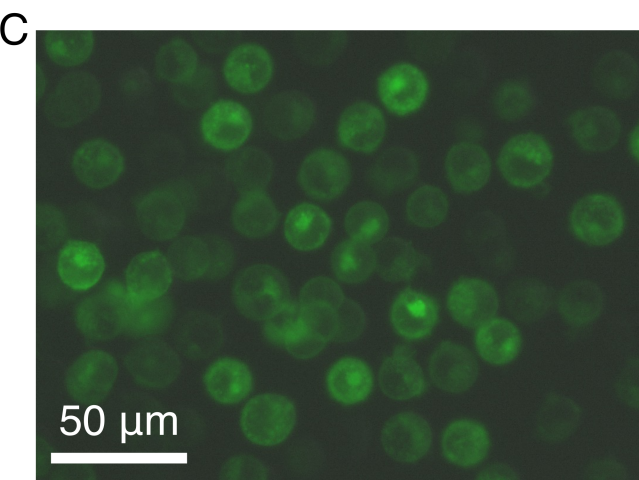
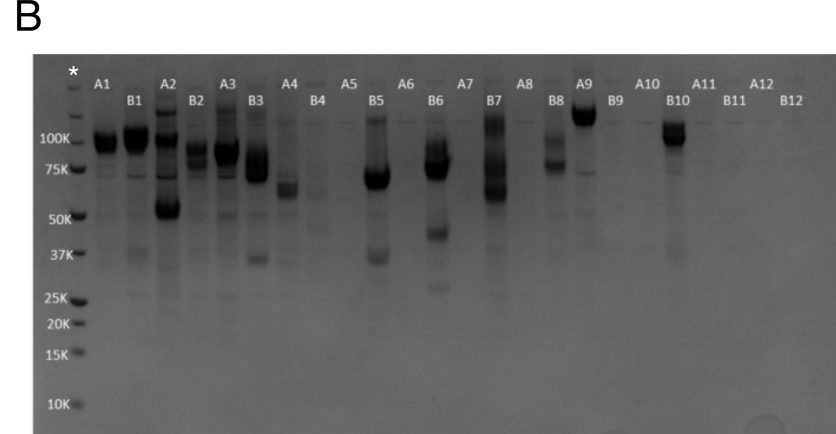
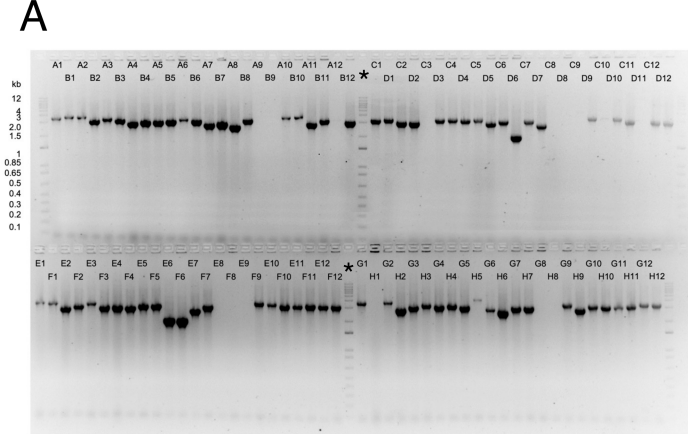
788 70. Zimmermann, I. et al. Synthetic single domain antibodies for the conformational trapping
789 of membrane proteins. *eLife*. **7**, e34317 (2018).

790 71. Yandrapalli, N., Robinson, T. Ultra-high capacity microfluidic trapping of giant vesicles for
791 high-throughput membrane studies. *Lab on a Chip*. **19** (4), 626–633 (2019).

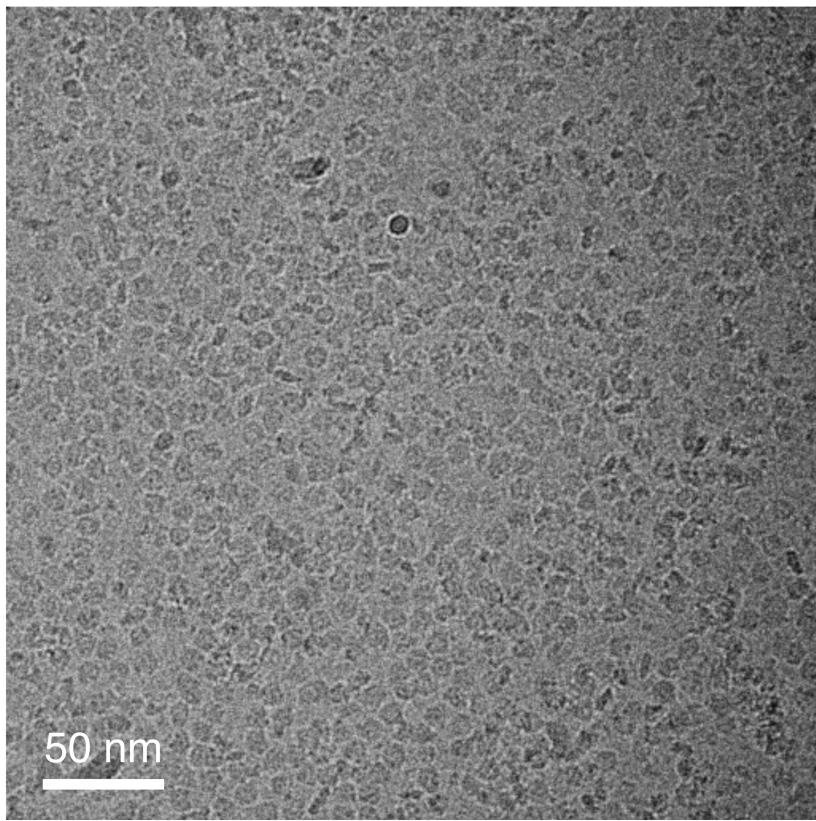
792 72. Bazzone, A., Barthmes, M., Fendler, K. SSM-based electrophysiology for transporter

793 research. *Methods in Enzymology*. **594**, 31–83 (2017).
794 73. Maynard, J. A. et al. Surface plasmon resonance for high-throughput ligand screening of
795 membrane-bound proteins. *Biotechnology Journal*. **4** (11), 1542–1558 (2009).
796 74. Haffke, M., Duckely, M., Bergsdorf, C., Jaakola, V. -P., Shrestha, B. Development of a
797 biochemical and biophysical suite for integral membrane protein targets: A review. *Protein*
798 *Expression and Purification*. **167**, 105545 (2020).
799
800

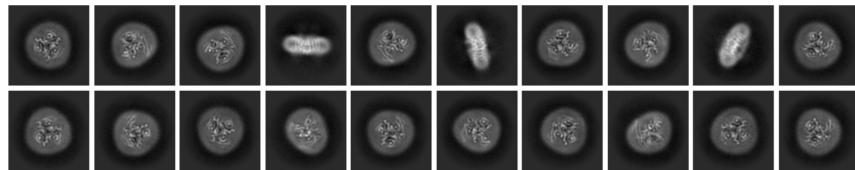




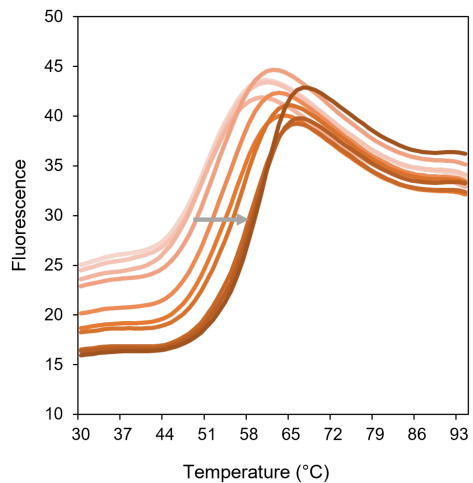
A



B



C



D

